NASA TECHNICAL NOTE

NASA TN D-3102

AMPTIAC

TWO-DIMENSIONAL HEAT TRANSFER IN RADIATING STAINLESS-STEEL-CLAD COPPER FINS

by Norbert O. Stockman and Edward C. Bittner

Lewis Research Center
Cleveland, Ohio

20060516238

TWO-DIMENSIONAL HEAT TRANSFER IN RADIATING

STAINLESS-STEEL-CLAD COPPER FINS

By Norbert O. Stockman and Edward C. Bittner

Lewis Research Center
Cleveland, Ohio

TWO-DIMENSIONAL HEAT TRANSFER IN RADIATING STAINLESS-STEEL-CLAD COPPER FINS

by Norbert O. Stockman and Edward C. Bittner

Lewis Research Center

SUMMARY

An analysis of the two-dimensional heat transfer in a radiating composite fin is presented together with details of the numerical method of solution. Several stainless-steel-clad copper fins typical of finned-tube space radiators are analyzed over a range (0 to 1) of stainless-steel to copper thickness ratio. Items discussed are temperature profiles along the fin length, temperature drop across fin thickness, effective conductivity, fin efficiency, heat rejection rate per unit weight, and ratio of effective conductivity to effective density. It was found for the particular geometries analyzed that the two-dimensional temperature distribution in the fin cross section is essentially one-dimensional. The use of the thickness-averaged conductivity in one-dimensional calculations yields essentially the same results as the two-dimensional calculations.

INTRODUCTION

The radiator of an electric-power generation system for space applications may account for a substantial portion of the powerplant total weight (refs. 1 and 2). An important factor in the minimum-weight design of these radiators is the selection of suitable materials (ref. 3). The large number of basic requirements (see ref. 3 for discussion) that must be satisfied makes the selection difficult. Often all the desirable qualities cannot be found in any one currently available material, and composite materials are therefore considered. In particular, the fin material for a space powerplant radiator should have a high value for the ratio of thermal conductivity to density (ref. 3), adequate strength, and a low sublimation rate in vacuum at high temperature. Stainless steel has adequate strength and satisfactory sublimation rate but low thermal conductivity, whereas copper has very high conductivity but questionable strength and sublimation rate at temperatures above about 800° K. These facts lead to a consideration of the composite material, stainless-steel-clad copper, for radiator fins (e.g., in the SNAP-50/SPUR design studies, refs. 4 and 5). Stainless-steel-clad copper has already been used in other applications (e.g., cooking utensils and heat exchangers) for several years and is commercially available. If a composite material is to be used for radiator fins, its effective thermal conductivity must be known for use in one-dimensional calculations for radiator design and comparison purposes. Suppliers of stainless-steel-clad copper material usually quote two values of effective conductivity: one value

for one-dimensional conduction in the direction parallel to the plane of the interface, and another value for one-dimensional conduction normal to the plane of the interface. For any significant thickness of clad these two values are quite different (e.g., for a stainless-steel to copper thickness ratio of only 0.05 these values are, respectively, 0.955 and 0.525 that of copper alone). In a radiator fin the conduction heat transfer is two-dimensional, and the value of effective conductivity will lie somewhere between the two one-dimensional values.
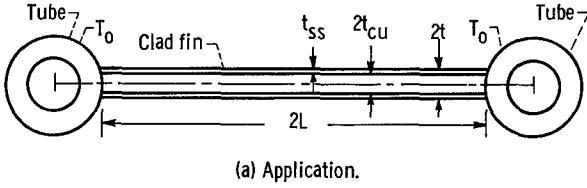
Specifically, the heat radiated by a fin is initially supplied across the fin thickness at the tube edge and is conducted parallel to the fin surface. The heat must subsequently reach the surface of the fin where it is radiated to space. There is clearly a two-dimensional effect involved, and the magnitude of this effect will increase as the stainless-steel to copper thickness ratio increases since the stainless steel has a much lower conductivity than copper. On the other hand, a radiator fin is usually very long relative to its thickness, which will tend to decrease the two-dimensional effect. Therefore, it is not a priori evident how great the two-dimensional effect will be, nor is it evident what the effective conductivity of a radiating fin will be.

Reference 6 attacks this type of problem in a quasi-two-dimensional way by assuming a one-dimensional heat flow in the fin core parallel to the radiating surface and one-dimensional heat flow in the clad or coating normal to the radiating surface. The primary application of the analysis of reference 6 is for coated fins having a relatively thin, very low conductivity, nonmetallic coating. The metallic-clad and the nonmetallic-coated fins present essentially the same problem. However, it is not obvious that the method of reference 6 will be adequate for metallic-clad fins in all cases because a metallic clad is thicker and has a higher value of thermal conductivity than a nonmetallic coating.

This report presents a brief analysis of the two-dimensional heat transfer in a composite fin with the conventional fin-tube radiator boundary conditions, that is, radiation from both surfaces and prescribed constant temperature at the fin base. An exact effective conductivity is obtained from the two-dimensional results and is compared with the conductivity for one-dimensional conduction in the direction parallel to the fin surface.

Several cases are analyzed that cover a range of the conductance parameter (the conventional identifying parameter for radiating fins). The range in this parameter is obtained by varying the length and thickness of the fin at two different temperature levels. For each case several values of stainless-steel to copper thickness ratio are prescribed. The results to be presented are discussed under two main headings: first, the degree of two-dimensionality of the several cases, and second, the effect of varying the conductance parameter and the stainless-steel to copper thickness ratio on fin temperature profiles, fin efficiency, heat rejected per unit weight, and effective conductivity to effective density ratio.
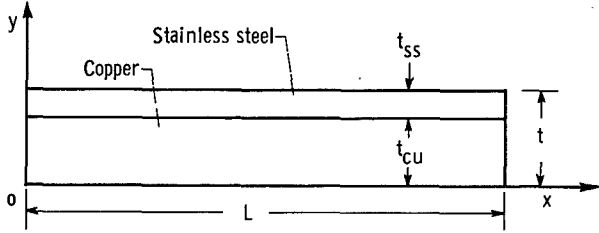
2

(a) Application.

(b) As considered in analysis (thickness exaggerated).

Figure 1. – Cross section of stainless-steel-clad copper fin.

The configuration to be analyzed is shown in figure 1. This is a stainless-steel-clad copper fin such as might be used in a central fin-tube radiator (fig. 1(a)). Only one quarter of the fin is analyzed (fig. 1(b)) because symmetry is assumed about x = L and y = 0. There is no heat flow across these boundaries. The temperature at x = 0 is assumed constant and equal to the tube outer-surface (base) temperature in a fin-tube configuration.

The analysis is based on steady-state two-dimensional conduction in the fin and the clad with perfect thermal contact at the interface ($y = t_{cu}$). The surface of the clad ($y = t$) is assumed to be radiating hemispherically at constant emittance to space, but radiant interchange with the tubes and incident radiation from the surroundings are neglected for simplicity. Also, the effective sink temperature of space is assumed to be zero. It is assumed that the thermal conductivity along the fin does not vary with temperature. For the range of variables considered herein the maximum error in assuming constant conductivity is estimated as less than 0.6 percent by the method of reference 7.

Basic Equations

The equation governing the two-dimensional conduction in the copper is

$$\frac{\partial^2 T_{cu}(x,y)}{\partial x^2} + \frac{\partial^2 T_{cu}(x,y)}{\partial y^2} = 0 \tag{1}$$

and in the stainless steel clad is

$$\frac{\partial^2 T_{ss}(x,y)}{\partial x^2} + \frac{\partial^2 T_{ss}(x,y)}{\partial y^2} = 0 \tag{2}$$

where $T_{cu}(x,y)$ is the local temperature in the fin and $T_{ss}(x,y)$ is the local temperature in the clad. (All symbols are defined in appendix A.)

At the boundary $y = t_{cu}$ between the fin and clad, perfect thermal contact is assumed:

$$T_{cu}(x,t_{cu}) = T_{ss}(x,t_{cu}) \tag{3}$$

Also at this boundary there must be continuity of heat flow; hence,

$$k_{cu}\left[\frac{\partial T_{cu}(x,y)}{\partial y}\right]_{y=t_{cu}} = k_{ss}\left[\frac{\partial T_{ss}(x,y)}{\partial y}\right]_{y=t_{cu}} \tag{4}$$

where k_{cu} is the thermal conductivity of the fin and k_{ss} that of the clad.

At the radiating surface $(y = t)$,

$$-k_{ss}\left[\frac{\partial T_{ss}(x,y)}{\partial y}\right]_{y=t} = \epsilon\sigma T_{ss}^4(x,t) \tag{5}$$

In accord with the assumptions mentioned previously, the equations for the remaining boundary conditions are

$$T_{cu}(x,y) = T_{ss}(x,y) = T_o \qquad x = 0$$

$$\left.\begin{array}{ll} \dfrac{\partial T_{cu}(x,y)}{\partial x} = \dfrac{\partial T_{ss}(x,y)}{\partial x} = 0 & x = L \\[3mm] & \\ \dfrac{\partial T_{cu}(x,y)}{\partial y} = 0 & y = 0 \end{array}\right\}\ \text{symmetry}$$

and

In order to facilitate comparison of the solutions for different cases, the following dimensionless parameters are formed:

(1) Clad-to-core thickness ratio, t_{ss}/t_{cu}

(2) Aspect ratio of copper fin, t_{cu}/L

(3) Conductivity ratio, k_{ss}/k_{cu}

(4) Temperature ratio, $\theta(X,Y) = T(x,y)/T_o$

(5) Distance ratio for any distance, $X = x/L$ and $Y = y/L$

(6) Conductance parameter, $\lambda = \epsilon\sigma T_o^3 L^2/k_{cu}t$

This last ratio does not occur naturally in the two-dimensional analysis of clad fins, but it is used because of its wide occurrence in fin-tube radiator literature.

Putting the dimensionless parameters into equations (1) and (2) yields the following:

In the fin:

$$\frac{\partial^2 \theta_{cu}(X,Y)}{\partial X^2} + \frac{\partial^2 \theta_{cu}(X,Y)}{\partial Y^2} = 0 \tag{6}$$

In the clad:

$$\frac{\partial^2 \theta_{ss}(X,Y)}{\partial X^2} + \frac{\partial^2 \theta_{ss}(X,Y)}{\partial Y^2} = 0 \tag{7}$$

The boundary conditions then become the following:

At $Y = \dfrac{t_{cu}}{L}$:

$$\theta_{cu}\left(X, \frac{t_{cu}}{L}\right) = \theta_{ss}\left(X, \frac{t_{cu}}{L}\right) \tag{8}$$

and

$$\frac{\partial \theta_{cu}(X,Y)}{\partial Y} = \frac{k_{ss}}{k_{cu}} \frac{\partial \theta_{ss}(X,Y)}{\partial Y} \tag{9}$$

At $Y = \dfrac{t}{L} = \dfrac{t_{cu}}{L}\left(1 + \dfrac{t_{ss}}{t_{cu}}\right)$:

$$\frac{\partial \theta_{ss}(X,Y)}{\partial Y} = -\lambda \frac{t_{cu}}{L} \frac{k_{cu}}{k_{ss}} \theta_{ss}^4\left(X, \frac{t}{L}\right) \tag{10}$$

At $X = 0$:

$$\theta_{ss}(X,Y) = \theta_{cu}(X,Y) = 1.0 \tag{11}$$

At $X = 1.0$:

$$\frac{\partial \theta_{ss}(X,Y)}{\partial X} = \frac{\partial \theta_{cu}(X,Y)}{\partial X} = 0 \tag{12}$$

At $Y = 0$:

$$\frac{\partial \theta_{cu}(X,Y)}{\partial Y} = 0 \tag{13}$$

It is thus seen that the independent parameters are t_{cu}/L, t_{ss}/t_{cu}, k_{ss}/k_{cu}, and λ, and their specification determines the temperature distribution throughout the fin. Results are given in dimensionless form in terms of these dimensionless variables; however, the calculations were made on the dimensional equa-

tions (1) and (2). These equations subject to the dimensional boundary conditions given previously were solved numerically on an IBM 7094 computer using a finite-difference, line-by-line, overrelaxation method. Details of the numerical method of solution are given in appendix B.

Fin Efficiency

A common measure of fin performance is the radiating efficiency, which is defined as the ratio of the actual heat radiated by the fin based on the calculated temperature distribution along the outer surface to the heat radiated by an isothermal fin at the base temperature T_O: that is,

$$\eta = \frac{Q}{Q_{ideal}} = \frac{\int_0^L \epsilon\sigma T_{ss}^4(x,t)\,dx}{\epsilon\sigma T_O^4 L} = \int_0^1 \theta_{ss}^4\left(X,\frac{t}{L}\right)\,dX \tag{14}$$

This parameter will be used to evaluate the effect of various thicknesses of clad.

Effective Thermal Conductivity

The effective conductivity of a clad fin is a function of the conductivities and the relative dimensions of the copper core and the stainless steel clad. It is also a function of the path the flow of heat must take to reach the radiating surface of the clad fin. These considerations are reflected in an effective conductivity $\bar{k}$ of clad fin which, in this report, is that value of conductivity that satisfies

$$\lambda_{eff} = \frac{\epsilon\sigma T_O^3 L^2}{\bar{k}t} \tag{15}$$

where λ_{eff} is that value of λ which, when used in one-dimensional radiating fin calculations (such as those of refs. 8 and 9 or the constant property cases of ref. 7), will result in the value of radiating efficiency η obtained herein by two-dimensional calculations.

RESULTS AND DISCUSSION

Several fin geometries representative of 300-kilowatt and 1-megawatt electrical-power-output Rankine-cycle space powerplants were analyzed. Two temperature levels (811° and 950° K) were chosen, and the fin length and fin thickness were varied to obtain a range of practical values of the identifying parameter λ. These input parameters are summarized in table I. Each basic configuration of table I was analyzed over a range of thickness ratios between 0 and 1. The variation in thickness ratio for a given configuration was ob-

TABLE I. - INPUT PARAMETERS[a]

[Emittance, ϵ, 0.9; thermal conductivity of copper, k_{cu}, 3.65 W/(cm)(°K); thermal conductivity of stainless steel, k_{ss}, 0.1818 W/(cm)(°K); conductivity ratio, k_{ss}/k_{cu}, 0.05.]

Case	Base temperature, T_o, °K	Fin length, L, cm	Copper fin thickness, t_{cu}, cm	Conductance parameter, λ	Aspect ratio of copper fin, t_{cu}/L
A	811	2.0	0.05	0.1218	0.0250
B		5.1	.20	.1904	.0400
C		4.1	.05	.4874	.0125
D		10.2	.20	.7616	.0200
E		5.6	.05	1.0000	.0089
F		15.3	.20	1.7136	.0131
G	950	1.8	0.05	0.1499	0.0286
H		4.3	.20	.2210	.0471
I		3.6	.05	.5996	.0143
J		8.6	.20	.8841	.0236
K		12.9	.20	1.9892	.0155

[a]To convert from cm to in., multiply by 0.3937; °K to °F, °F = 9/5 °K - 460; °K to °R, multiply by 9/5; W/(cm)(°K) to Btu/(hr)(ft)(°R), multiply by 57.8.

Figure 2. - Surface temperature distribution of cases A and K for thickness ratios from 0 to 1.0.

tained by decreasing t_{cu}, the thickness of copper, and increasing t_{ss}, the thickness of stainless steel clad, while maintaining a constant total thickness t. The conductivity ratio k_{ss}/k_{cu} should be a function of fin-base temperature; however, to reduce the number of parameters, the same value was used for both temperature levels.

The results to be presented are discussed under two main headings: first, the degree of two dimensionality present in the cases analyzed, and second, the effect on certain fin parameters of varying the stainless-steel to copper thickness ratio.

Degree of Two-Dimensionality

The items to be discussed in this section are temperature profiles along the fin length,
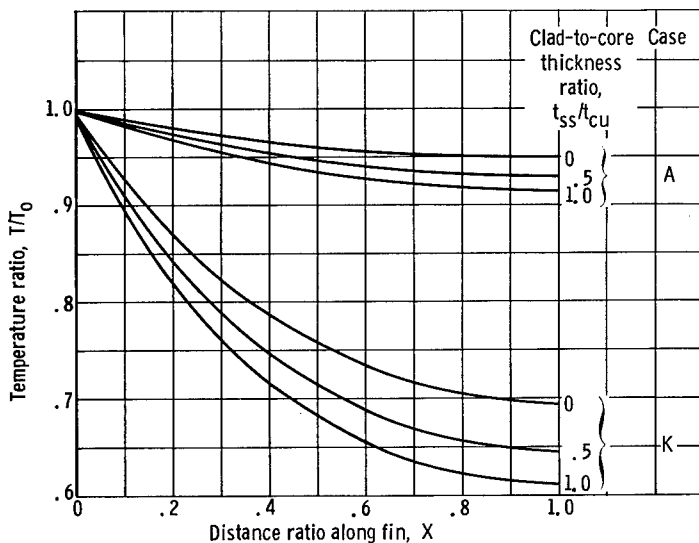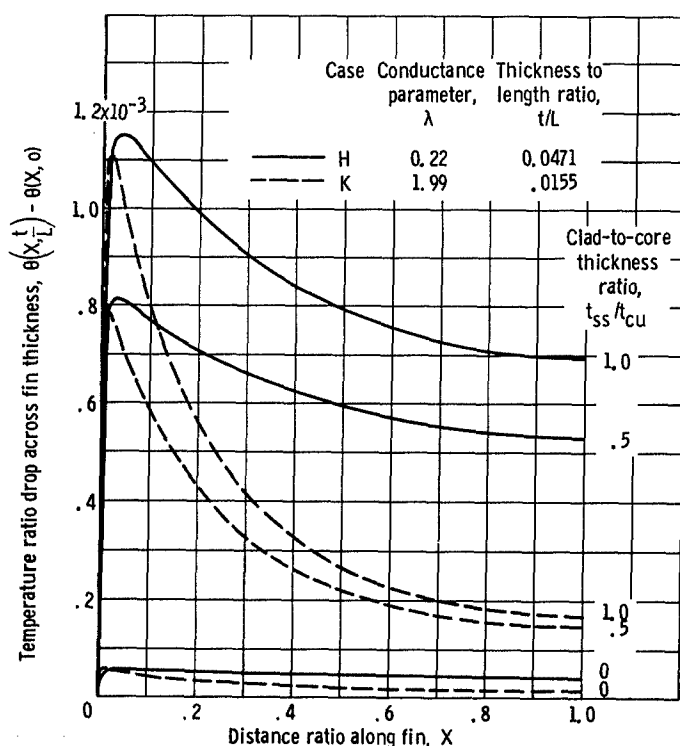
Figure 3. - Temperature ratio drop across fin thickness against distance ratio along fin.

temperature drop across the fin thickness, effective conductivity, and comparison of two-dimensional and one-dimensional results.

Temperature drop across fin. - Of the several cases analyzed (table I), case A has the smallest temperature gradient along the fin length and case K has the largest. The temperature profiles of these two extreme cases at three values of thickness ratio t_{ss}/t_{cu} are shown in figure 2. The two-dimensional effect, that is, the difference between the temperature profile along the radiating surface of the fin $(Y = t/L)$ and that along the adiabatic surface $(Y = 0)$, is not large enough to be seen on the scale of figure 2.

The two-dimensional effect is shown more specifically on figure 3 in the form of the temperature ratio drop across the fin from $Y = 0$ to $Y = t/L$ for three values of t_{ss}/t_{cu}. The cases shown are case K, because it has the steepest X-direction temperature gradient (fig. 2), and case H, because it has the largest Y-direction temperature gradient. The variation in t_{ss}/t_{cu} was obtained by reducing t_{cu} and increasing t_{ss} to maintain a constant total thickness t. The clad fins have a greater two-dimensional effect than the all-copper fins $(t_{ss}/t_{cu} = 0)$ as shown in the figure. It should be noted, however, that the scale of the ordinate in figure 3 is greatly expanded and the maximum difference in temperature ratio between the fin centerline and the fin surface is only about 1.15×10^{-3} unit.

Effective conductivity. - As was stated in the INTRODUCTION the value of effective conductivity of a radiating clad fin should lie somewhere between the one-dimensional value for conduction in the direction parallel to the fin surface and that for conduction normal to the surface. In view of the small two-dimensional effect noted in the previous section, it is to be expected that the effective conductivity of the radiating fin would be close to that for one-dimensional conduction in the parallel or x-direction. To check this expectation, the exact effective conductivity for the two-dimensional radiating fin will be investigated and will then be compared with the one-dimensional x-direction conductivity.

An exact value of effective conductivity can be obtained from equation (15). Solving equation (15) for the exact effective conductivity $\bar{k}$ and forming the ratio $\bar{k}/k_{cu}$ yield
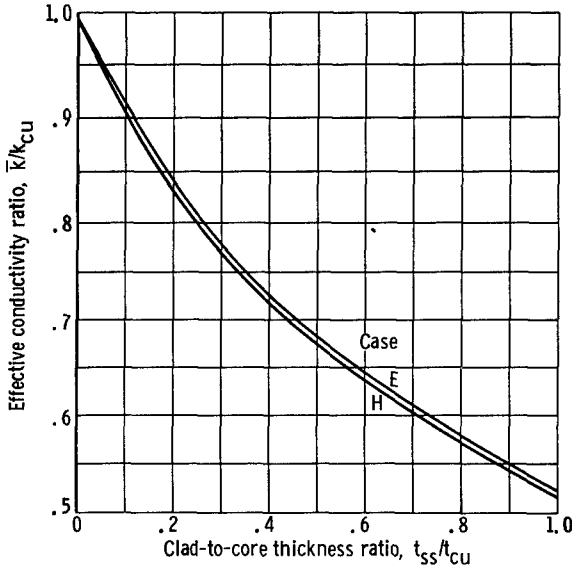
Figure 4. - Exact effective conductivity ratio against thickness ratio.

$$\frac{\overline{k}}{k_{cu}} = \frac{\epsilon \sigma T_O^3 L^2}{t k_{cu} \lambda_{eff}} \qquad (16)$$

The grouping $\epsilon \sigma T_O^3 L^2 / t k_{cu}$ of equation (16) is equal to the conductance parameter λ. Substituting λ into equation (16) yields

$$\frac{\overline{k}}{k_{cu}} = \frac{\lambda}{\lambda_{eff}} \qquad (17)$$

A value of λ_{eff} was obtained from one-dimensional calculations for each value of η obtained from the two-dimensional calculations reported herein, and the effective conductivity ratio was obtained from equation (17). On figure 4 are shown curves for the exact radiating-fin effective conductivity ratio $\overline{k}/k_{cu}$ as a function of thickness ratio t_{ss}/t_{cu} for cases E and H. The remaining cases listed in table I fall between these two curves and are omitted for clarity. The close agreement among the several cases indicates that the effective conductivity ratio $\overline{k}/k_{cu}$ is dependent primarily on thickness ratio t_{ss}/t_{cu} for a given conductivity ratio k_{ss}/k_{cu}. The exact value of effective conductivity will be compared with the effective conductivity based on one-dimensional conduction in the x-direction, which is the thickness-averaged value given by

$$\overline{k}_x = \frac{t_{ss} k_{ss} + t_{cu} k_{cu}}{t_{ss} + t_{cu}} \qquad (18)$$

Writing equation (18) in terms of dimensionless ratios yields

$$\frac{\overline{k}_x}{k_{cu}} = \frac{\dfrac{t_{ss}}{t_{cu}} \dfrac{k_{ss}}{k_{cu}} + 1}{1 + \dfrac{t_{ss}}{t_{cu}}} \qquad (19)$$

Thus, the ratio $\overline{k}_x/k_{cu}$ is a function only of the thickness ratio t_{ss}/t_{cu} and the conductivity ratio k_{ss}/k_{cu}. The relation between $\overline{k}_x/k_{cu}$ and t_{ss}/t_{cu} is shown on figure 5(a) for a conductivity ratio k_{ss}/k_{cu} of 0.05. Also plotted in figure 5(a) is the exact effective conductivity ratio of the case that deviates most from the thickness-averaged conductivity (case H). The close agreement between $\overline{k}_x/k_{cu}$ and $\overline{k}/k_{cu}$ is evident.

As was stated earlier, only one value of k_{ss}/k_{cu} was used even though two temperature levels were considered. To determine whether the change in
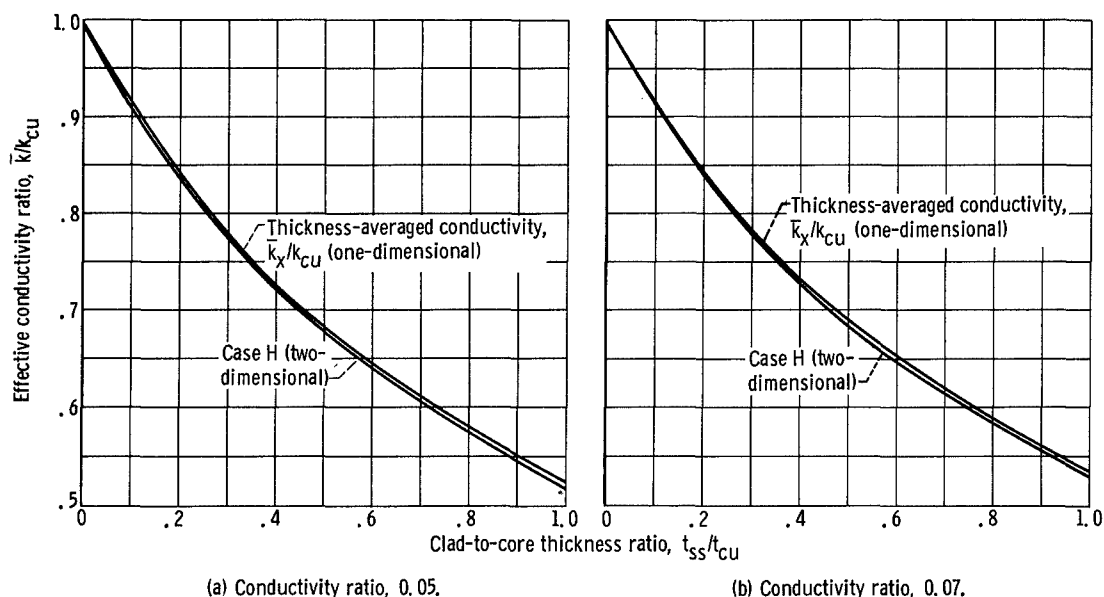
9

(a) Conductivity ratio, 0.05.　　　　　　　　(b) Conductivity ratio, 0.07.

Figure 5. - Comparison of thickness-averaged conductivity with exact two-dimensional effective conductivity.

k_{ss}/k_{cu} over the temperature range of interest significantly affected the agreement of $\bar{k}/k_{cu}$ and $\bar{k}_x/k_{cu}$, case H was analyzed with a conductivity ratio k_{ss}/k_{cu} of 0.07 (corresponding to a temperature of 911° K). The results are shown in figure 5(b), and the agreement is seen to be not significantly different from that of figure 5(a).

This close agreement of $\bar{k}_x/k_{cu}$ with $\bar{k}/k_{cu}$ means that the thickness-averaged effective conductivity can safely be used in radiator heat-transfer calculations for geometries comparable to those treated herein.

Comparison of one-dimensional and two-dimensional results. - As a further check of the closeness between the results of one-dimensional calculations with the thickness-averaged conductivity $\bar{k}_x$ and the two-dimensional solutions, several cases were analyzed by the method of reference 7 but with constant properties. (The one-dimensional methods of refs. 8 or 9 could also be used.) The cases chosen from table I were those having extreme values of λ, cases A and K, and those having extreme values of t/L, cases E and H (case H has the greatest two-dimensional effect). In all cases the temperature profiles and fin efficiencies agreed with the two-dimensional results to within three places with small variations in the fourth place. Thus, for the range of λ, t/L, and t_{ss}/t_{cu} treated herein, the use of thickness-averaged conductivity in one-dimensional calculations will give essentially the same results as the more exact two-dimensional calculations.

Effect of Varying Thickness Ratio

The stainless-steel to copper thickness ratio used will in general depend on the particular application. All the cases of table I were analyzed with thickness ratios t_{ss}/t_{cu} of 0, 0.1, 0.3, 0.5, and 1.0. The effect of this
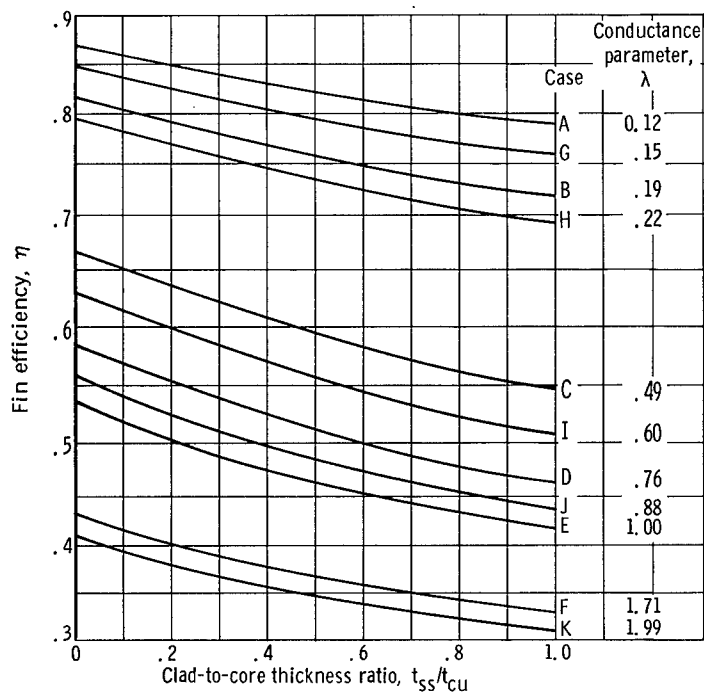
Figure 6. - Fin efficiency against thickness ratio for cases with constant total fin thickness.
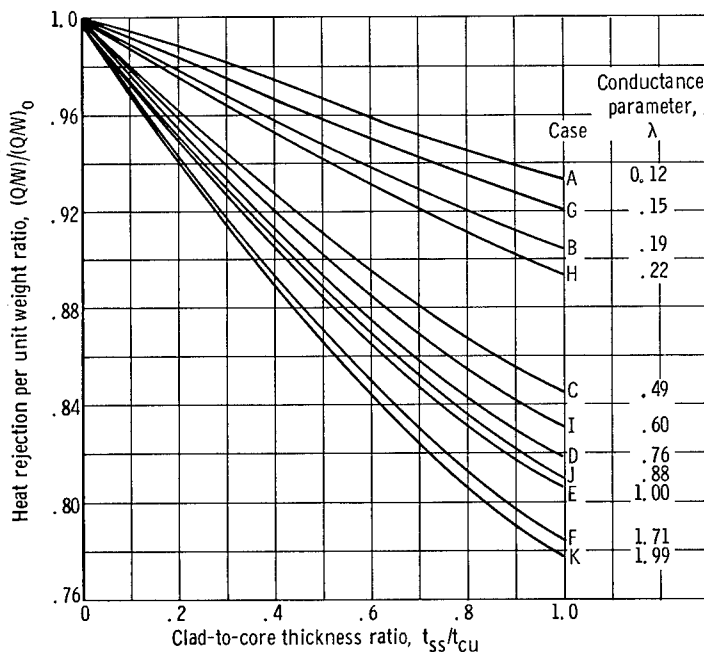

Figure 7. - Heat rejection per unit weight ratio against thickness ratio.

variation in thicknsss ratio on several parameters used in evaluating fins or fin materials is presented in this section. Most of the results presented were obtained from the same two-dimensional calculations as the temperature profiles presented previously. Essentially the same results could also have been obtained from one-dimensional calculations because of the close agreement noted in the preceding section.

Fin efficiency. - The effect on fin efficiency η of varying t_{ss}/t_{cu} is shown on figure 6. This figure indicates a significant drop in heat transfer as the high conductivity copper is replaced by the lower conductivity steel. Thus, making the simplest assumption and treating the clad as if it were copper would introduce a large heat rejection error in radiator calculations (except for very small t_{ss}/t_{cu}). For example, for case K ($\lambda = 1.99$) with $t_{ss}/t_{cu} = 0.5$, the fin efficiency is 16 percent lower than that for the all copper fin ($t_{ss}/t_{cu} = 0$). However, as was indicated earlier, the clad fin can be treated accurately in one-dimensional radiator calculations with the use of the thickness-averaged (effective) conductivity.

Heat rejection rate per unit weight. - An important parameter used for comparative evaluation of a radiator component is the heat rejection rate per unit weight Q/W. Therefore, to study the effect of varying the proportion of stainless steel to copper in a clad fin the ratio $(Q/W)/(Q/W)_o$ is formed, where $(Q/W)_o$ is the Q/W for an all copper fin ($t_{ss}/t_{cu} = 0$). This
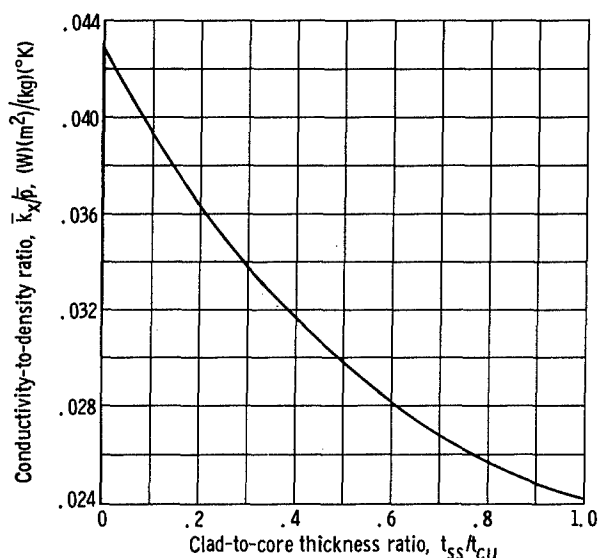
11

Figure 8. - Ratio of effective conductivity to effective density against thickness ratio.

ratio is plotted in figure 7 as a function of t_{ss}/t_{cu}. For most practical radiators, t_{ss}/t_{cu} will be less than 0.5, and consequently the reduction in Q/W will vary between 3 and 14 percent for values of λ ranging between 0.12 and 2.0, respectively. However, this is the effect on the fin only. The net effect of using clad fins on the total radiator Q/W will depend on the relative contributions of the fins to total radiator weight and in many cases will be less than the effect shown in figure 7.

Conductivity to density ratio. - A parameter based on material properties that is used to compare the conducting capabilities of materials on a weight basis is k/ρ (ref. 3). To compare stainless-steel-clad copper on this basis, the ratio $\overline{k}_x/\overline{\rho}$ is formed, where $\overline{\rho}$ is the average density of the clad fin and is given by

$$\overline{\rho} = \frac{t_{ss}\rho_{ss} + t_{cu}\rho_{cu}}{t_{ss} + t_{cu}} \qquad (20)$$

and $\overline{k}_x$ is the thickness-averaged conductivity defined previously in equation (18).

TABLE II. - CONDUCTIVITY TO DENSITY RATIO[a] FOR

SEVERAL MATERIALS AT 811° K

Material	Conductivity to density ratio, $\overline{k}_x/\overline{\rho}$ $(W)(m^2)/(kg)(°K)$
Pyrolytic graphite	0.132
Beryllium	.0583
Commercial graphite	.0550
Copper, $t_{ss}/t_{cu} = 0$	.0428
Stainless-steel-clad copper, $t_{ss}/t_{cu} = 0.5$	.0308
Stainless-steel-clad copper, $t_{ss}/t_{cu} = 1.0$	.0231
Molybdenum	.0132
Columbium	.0077
Tantalum	.00385
Titanium	.00385
Stainless steel	.00286
Vanadium	.00231

[a]All data except stainless-steel-clad copper obtained from fig. 9 of ref. 3.

The ratio $\overline{k}_x/\overline{\rho}$ is plotted against t_{ss}/t_{cu} in figure 8. In table II these values of $\overline{k}_x/\overline{\rho}$ are compared with the k/ρ values obtained for a variety of materials from reference 3. It can be seen that for thickness ratios up to 0.5, stainless-steel-clad copper has a higher $\overline{k}/\overline{\rho}$ value than most of the materials listed, and is not too far removed from the best materials.

SUMMARY OF RESULTS

For the particular configurations analyzed the following results have been obtained:

1. The temperature in the clad fin shows only a slight two-dimensional effect.

2. The effective conductivity of a radiating clad fin is very nearly equal to the thickness-averaged conductivity (one-dimensional) of the clad fin.

3. One-dimensional calculations that use the thickness-averaged conductivity yield essentially the same results for temperature profile and fin effectiveness as the two-dimensional calculations.

4. Increasing the proportion of stainless steel in a clad fin of given total thickness decreases the radiating effectiveness of the fin. For a stainless-steel to copper thickness ratio of 0.5, the reduction is 16 percent.

5. The ratio of effective conductivity to effective density of a stainless-steel-clad copper fin is relatively high and remains competitive with the other materials of interest.

Lewis Research Center,
        National Aeronautics and Space Administration,
            Cleveland, Ohio, August 17, 1965.

APPENDIX A

SYMBOLS

$\mathscr{A}$	matrix of system of finite-difference equations
a	diagonal elements of matrix $\mathscr{B}$
$\mathscr{B}$	submatrices of order NY of $\mathscr{A}$ which lie along the diagonal
b	off-diagonal elements of matrix $\mathscr{B}$
$\mathscr{C}$	off-diagonal submatrix of order NY of $\mathscr{A}$
c	elements of matrix $\mathscr{C}$
$\vec{d}$	vector whose components are right-hand sides of finite-difference equation
I	position number of horizontal grid line
J	position number of vertical grid line
k	thermal conductivity, $W/(cm)(^\circ K)$
$\bar{k}$	effective conductivity of radiating clad fin, $W/(cm)(^\circ K)$
$\bar{k}_x$	effective conductivity of clad fin transferring heat by conduction in x-direction only, $W/(cm)(^\circ K)$
L	fin length, cm
m	number of current iteration
NDX	number of vertical grid strips
NDYC	number of horizontal grid strips in clad
NDYF	number of horizontal grid strips in fin
NX	total number of vertical grid lines
NY	total number of horizontal grid lines
n	distance normal to surface, cm
Q	heat rejection rate, $W/(cm)(sec)$
Q_{ideal}	heat rejection rate of an isothermal fin at temperature T_o, $W/(cm)(sec)$

14

s	distance along a surface, cm
T	temperature, $^\circ K$
$\vec{T}$	vector of temperatures
$\vec{\tilde{T}}$	vector of temperatures, intermediate in the computation
t	thickness, cm
W	fin weight, kg
X	x/L
x	distance along length of fin, cm
Δx	grid spacing in x-direction, cm
Y	y/L
y	distance along thickness of fin, cm
Δy	grid spacing in y-direction, cm
$\vec{z}$	dummy variable vector
z_i	components of $\vec{z}$
α_i	coupling parameters (eq. (B15)) in difference equations
ϵ	emittance
η	radiating efficiency of fin
θ	temperature ratio, T/T_O
λ	conductance parameter, $\epsilon \sigma T_O^3 L^2 / k_{cu} t$
λ_{eff}	λ of clad fin, $\epsilon \sigma T_O^3 L^2 / \bar{k} t$
$\vec{\mu}$	vector of ratio of elements of the matrix $\mathscr{B}$
μ_i	components of $\vec{\mu}$
ρ	density, kg/m^3
$\bar{\rho}$	thickness-averaged density, kg/m^3
σ	Stefan-Boltzmann constant, 5.67×10^{-8} $W/(m^2)(^\circ K^4)$
ω	block-successive overrelaxation parameter

ω_b optimum value of ω

Subscripts:

cu   copper fin

J   variable horizontal position along fin

NX   last horizontal position along fin

NY   last vertical position on fin

o   value at $x = 0$ or $t_{ss}/t_{cu} = 0$

ss   stainless steel clad

Superscripts:

(m) m^{th} iterate

(o)   initial approximation

NUMERICAL APPROXIMATION OF TEMPERATURE DISTRIBUTION

Equations (1) and (2) may be replaced by the single equation

$$\frac{\partial}{\partial x}\left(k\ \frac{\partial T}{\partial x}\right) + \frac{\partial}{\partial y}\left(k\ \frac{\partial T}{\partial y}\right) = 0 \tag{B1}$$

which holds in the entire fin as a partial differential equation with discontinuous coefficients. Such problems have been treated recently (e.g., ref. 10). To solve equation (B1) subject to the boundary conditions, a rectangular grid is superimposed on the composite rectangle above the x-axis of figure 1(b) (p.3) in such a way that each boundary (including the interface) is a grid line, Δx is a constant L/NDX where NDX is the number of vertical strips laid off in the rectangle by the discretization, and Δy is one constant in the fin $\Delta y_{cu} = t_{cu}/NDYF$ and another in the clad $\Delta y_{ss} = t_{ss}/NDYC$. The grid points are labeled with ordered pairs (I,J) of positive integers in the manner to be described.

Let $NY = NDYF + NDYC + 1$ be the total number of horizontals in the grid. Number these $1, 2 \ldots NY$ starting at the lowermost ($y = 0$). Let $NX = NDX + 1$ be the number of verticals in the grid. Number these $1, 2 \ldots NX$ from left to right starting at the leftmost ($x = 0$). The first element of the ordered pair (I,J) is the position number of the horizontal and the second element is that of the vertical; thus, (I,J) is such that $1 \leq I \leq NY$ and $1 \leq J \leq NX$.

Next the partial differential equations and boundary conditions are replaced by a system of algebraic equations (some of which are nonlinear) obtained by integrating the partial differential equation over the cells of the "dual grid" (ref. 11, p. 11), by applying the divergence theorem, and by replacing the normal derivatives occurring in the boundary integrals by difference quotients, zero or $-\epsilon\sigma T^4$, depending on the position of the cell in question (ref. 12, sec. 6.3).

This process is illustrated by the following example taken at the point $x = \Delta x$, $y = t$ (i.e., $(I,J) = (NY,2)$). The cell in question of the dual grid (shaded in fig. 9) has its boundaries (except the upper one) midway between grid lines of the original grid. The algebraic equation at $(NY,2)$ is obtained in the following steps.

$$0 = \iint_{Cell} \left[\frac{\partial}{\partial x}\left(k\ \frac{\partial T}{\partial x}\right) + \frac{\partial}{\partial y}\left(k\ \frac{\partial T}{\partial y}\right)\right]dx\ dy$$

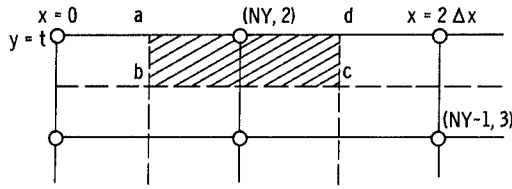$$0 = \oint_{\substack{Around \\ cell}} k\ \frac{\partial T}{\partial n}\ ds$$

Figure 9. - Detail of grid for numerical solution.

$$0 = \int_{a \to b} k_{ss} \left(-\frac{\partial T}{\partial x} \right) ds + \int_{b \to c} k_{ss} \left(-\frac{\partial T}{\partial y} \right) ds$$

$$+ \int_{c \to d} k_{ss} \frac{\partial T}{\partial x} ds + \int_{d \to a} k_{ss} \frac{\partial T}{\partial y} ds$$

$$0 \approx k_{ss} \left[\frac{T_0 - T(NY,2)}{\Delta x} \right] \frac{\Delta y_{ss}}{2} + k_{ss} \left[\frac{T(NY-1,2) - T(NY,2)}{\Delta y_{ss}} \right] \Delta x$$

$$+ k_{ss} \left[\frac{T(NY,3) - T(NY,2)}{\Delta x} \right] \frac{\Delta y_{ss}}{2} - \epsilon \sigma T^4(NY,2) \Delta x \qquad (B2)$$

This particular point was chosen to illustrate the fact that sometimes a path length in the integration is only one-half a total mesh width $(\Delta y_{ss}/2)$ and to illustrate the ease of handling the two types of boundary conditions inherent in this method of discretization (note first and fourth terms).

Repeating the integration on all cells that surround the points (I,J), $1 \leq I \leq NY$ and $2 \leq J \leq NX$, yields a system of $NY(NX - 1)$ equations (of which $NX - 1$ are nonlinear, viz., (NY,J), $2 \leq J \leq NX$) in as many unknowns $T(I,J)$. It is noted that $T(I,1) = T_0$ when $1 \leq I \leq NY$.

A direct solution of this system is impossible because of the nonlinearity; therefore, an iterative procedure must be used. Let $T^{(m)}(I,J)$ represent the mth iterate for $T(I,J)$ where $T^{(0)}(I,J)$ is some initial approximation to $T(I,J)$. Equations at the points (NY,J), $2 \leq J \leq NX$, are linearized in the same way that Newton's method for finding the roots of equations is derived (see ref. 13, p. 192). The term $\left[T^{(m)}(NY,J) \right]^4$ is replaced by the first two terms in its Taylor expansion about $T^{(m-1)}(NY,J)$, that is by

$$\left[T^{(m-1)}(NY,J) \right]^4 + 4\left[T^{(m-1)}(NY,J) \right]^3 \left[T^{(m)}(NY,J) - T^{(m-1)}(NY,J) \right]$$

which reduces to

$$4\left[T^{(m-1)}(NY,J) \right]^3 T^{(m)}(NY,J) - 3\left[T^{(m-1)}(NY,J) \right]^4$$

The resulting system of equations linear in $T^{(m)}$ can be written in matrix notation as

$$\mathscr{A} \vec{T}^{(m)} = \vec{d} \qquad (B3)$$

where

$$\mathscr{A} = \mathscr{A}\left[\vec{T}^{(m-1)} \right] \qquad (B4)$$

is a square matrix of order $NY(NX - 1)$ and

$$\vec{d} = \vec{d}\left(\vec{T}^{(m-1)}\right) \tag{B5}$$

is a column vector with $NY(NX - 1)$ components. $\mathscr{A}$ is a block tridiagonal matrix, that is,

$$\mathscr{A} = \begin{pmatrix} \mathscr{B}_2 & -\mathscr{C} & 0 & \cdots & & 0 & 0 \\ -\mathscr{C} & \mathscr{B}_3 & -\mathscr{C} & \cdots & & 0 & 0 \\ 0 & -\mathscr{C} & \mathscr{B}_4 & \cdots & & 0 & 0 \\ \cdot & \cdot & \cdot & \cdot\cdot\cdot & & \cdot & \cdot \\ \cdot & \cdot & \cdot & \cdot\cdot\cdot & & \cdot & \cdot \\ \cdot & \cdot & \cdot & \cdot\cdot\cdot & & \cdot & \cdot \\ 0 & 0 & 0 & \cdots & & \mathscr{B}_{NX-1} & -\mathscr{C} \\ 0 & 0 & 0 & \cdots & & -\mathscr{C} & \mathscr{B}_{NX} \end{pmatrix} \tag{B6}$$

Here

$$\mathscr{B}_J = \mathscr{B}\left(T^{(m-1)}(NY,J)\right) \qquad 2 \leq J \leq NX - 1 \tag{B7}$$

are square, tridiagonal matrices of order NY, all of whose elements are constant (independent of both J and $\vec{T}^{(m-1)}$) except for the element in the NY,NY position which depends on $T^{(m-1)}(NY,J)$. The remaining matrix on the diagonal of $\mathscr{A}$ is

$$\mathscr{B}_{NX} = \frac{1}{2}\mathscr{B}\left(T^{(m-1)}(NY,NX)\right) \tag{B8}$$

and $\mathscr{C}$ is a diagonal matrix (constant) of order NY. The iterative method may be described as a line-by-line (vertical) overrelaxation scheme, which is carried out in the following way.

An initial approximation to the temperature is taken at all points (e.g., $T^{(o)}(I,J) = T_O$). The temperatures are changed by sweeping through them from left to right an entire vertical at one time; the sweep is repeated if the convergence criterion has not been met. If attention is focused on the Jth vertical, the change is carried out by the following formulas. Let

$$\vec{T}_J^{(m)} = \begin{pmatrix} T^{(m)}(1,J) \\ \cdot \\ \cdot \\ \cdot \\ T^{(m)}(NY,J) \end{pmatrix} \tag{B9}$$

be the vector of temperatures along the Jth vertical at the mth iterate. It is assumed that $\vec{T}_{J-1}^{(m)}$ has already been computed and $\tilde{\vec{T}}_J^{(m)}$ defined by

$$\mathscr{B}_J \tilde{\vec{T}}_J^{(m)} = \mathscr{C}\left[\vec{T}_{J-1}^{(m)} + \vec{T}_{J+1}^{(m-1)}\right] \tag{B10}$$

Start

Figure 10. - Computer flow diagram.

where $\mathcal{B}_J$ is stored in computer memory in partially factored form since $\mathcal{B}_J$ is tridiagonal and almost constant. Therefore the computation of $\tilde{\vec{T}}_J$ is only a matter of a correction to the right-hand side and a back substitution. Then,

$$\vec{T}_J(m) = \vec{T}_J(m-1) + \omega\left[\tilde{\vec{T}}_J(m) - \vec{T}_J(m-1)\right]$$

(B11)

where ω is the "block successive overrelaxation parameter" (ref. 12, ch. 4) that controls the rate of convergence, and

$$0 < \omega < 2 \qquad (B12)$$

To further clarify this, the computation (eq. (B10)) on the second vertical ($J = 2$) is examined in detail, and reference is made to the block diagram of the computer program (fig. 10).
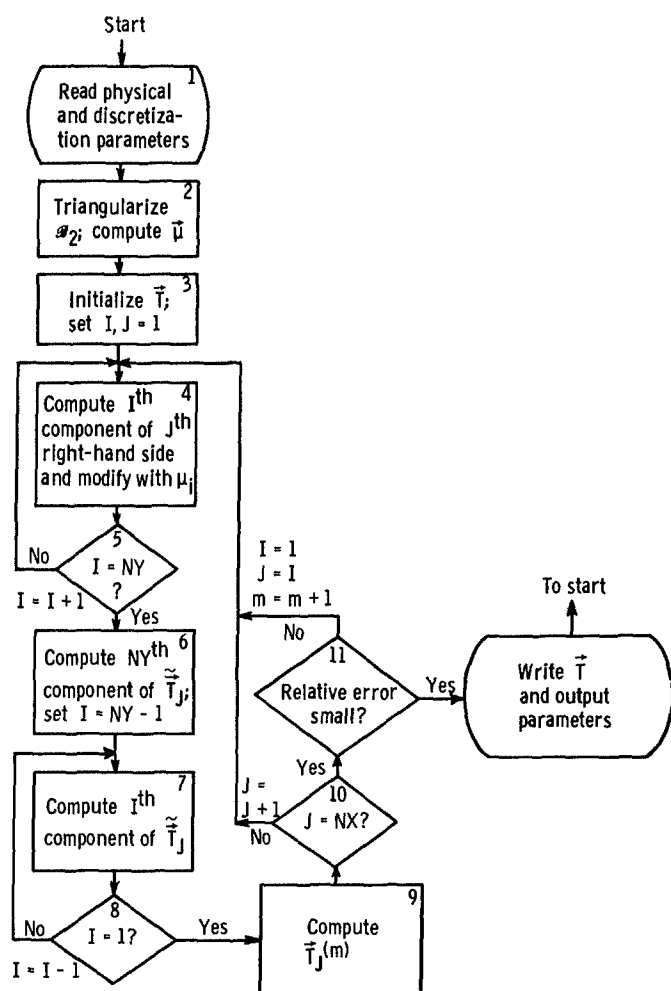
For $J = 2$,

$$\mathcal{B}_2 = \begin{pmatrix} a_1 & -b_1 & 0 & \cdots & 0 & 0 & 0 \\ -b_1 & a_2 & -b_2 & \cdots & 0 & 0 & 0 \\ 0 & -b_2 & a_3 & \cdots & 0 & 0 & 0 \\ \cdot & \cdot & \cdot & \cdots & \cdot & \cdot & \cdot \\ \cdot & \cdot & \cdot & \cdots & \cdot & \cdot & \cdot \\ \cdot & \cdot & \cdot & \cdots & \cdot & \cdot & \cdot \\ 0 & 0 & 0 & \cdots & a_{NY-2} & -b_{NY-2} & 0 \\ 0 & 0 & 0 & \cdots & -b_{NY-2} & a_{NY-1} & -b_{NY-1} \\ 0 & 0 & 0 & \cdots & 0 & -b_{NY-1} & a_{NY} \end{pmatrix}$$

(B13)

and

$$\mathcal{C} = \text{diag}(c_1 \cdots c_{NY}) \qquad (B14)$$

20

For convenience, define

$$\alpha_1 = \frac{\Delta y_{ss} k_{ss}}{\Delta x}$$

$$\alpha_2 = \frac{\Delta y_{cu} k_{cu}}{\Delta x}$$

$$\alpha_3 = \frac{\Delta x k_{ss}}{\Delta y_{ss}}$$

$$\alpha_4 = \frac{\Delta x k_{cu}}{\Delta y_{cu}}$$

(B15)

Then, when equation (B2) and analogous equations for the other points on this vertical are considered, the elements of $\mathscr{B}_2$ and $\mathscr{C}$ can be written as follows:

$$a_i = \begin{cases} \alpha_2 + \alpha_4 & i = 1 \\ 2(\alpha_2 + \alpha_4) & i = 2 \ldots \text{NDYF} \\ \alpha_1 + \alpha_2 + \alpha_3 + \alpha_4 & i = \text{NDYF} + 1 \\ 2(\alpha_1 + \alpha_3) & i = \text{NDYF} + 2 \ldots \text{NY} - 1 \\ \alpha_1 + \alpha_3 + 4\epsilon\sigma \, \Delta x \left[T^{(m-1)}(\text{NY},J) \right]^3 & i = \text{NY} \end{cases}$$

$$b_i = \begin{cases} \alpha_4 & i = 1 \ldots \text{NDYF} - 1 \\ \alpha_3 & i = \text{NDYF} \ldots \text{NY} - 1 \end{cases}$$

(B16)

$$c_i = \begin{cases} \alpha_2/2 & i = 1 \\ \alpha_2 & i = 2 \ldots \text{NDYF} \\ (\alpha_1 + \alpha_2)/2 & i = \text{NDYF} + 1 \\ \alpha_1 & i = \text{NDYF} + 2 \ldots \text{NY} - 1 \\ \alpha_1/2 & i = \text{NY} \end{cases}$$

Therefore, with equation (B10) rewritten for $J = 2$ as

$$\mathscr{B}_2 \vec{\tilde{T}}_2^{(m)} = \mathscr{C}\left[\vec{T}_1^{(m)} + \vec{T}_3^{(m-1)} \right]$$

the computation for $\vec{\tilde{T}}_2^{(m)}$ is carried out by solving the following system of equations where, for brevity, the vector

$$\vec{z} = \begin{pmatrix} z_1 \\ \cdot \\ \cdot \\ \cdot \\ z_{NY} \end{pmatrix} \tag{B17}$$

replaces the vector $\overset{\approx}{\vec{T}}_2^{(m)}$:

$$\left.\begin{aligned}
a_1 z_1 - b_2 z_2 \qquad\qquad\qquad &= c_1[T_o + T(1,3)] \\
-b_1 z_1 + a_2 z_2 - b_2 z_3 \qquad\qquad &= c_2[T_o + T(2,3)] \\
- b_2 z_2 + a_3 z_3 - b_3 z_4 \qquad &= c_3[T_o + T(3,3)] \\
\cdot \quad \cdot \quad \cdot \quad \cdot \qquad &\quad \cdot \quad \cdot \quad \cdot \\
\cdot \quad \cdot \quad \cdot \quad \cdot \qquad &\quad \cdot \quad \cdot \quad \cdot \\
-b_{NY-2} z_{NY-2} + a_{NY-1} z_{NY-1} - b_{NY-1} z_{NY} &= c_{NY-1}[T_o + T(NY-1,3)] \\
- b_{NY-1} z_{NY-1} + a_{NY} z_{NY} &= c_{NY}[T_o + T(NY,3)]
\end{aligned}\right\} \tag{B18}$$

Here the superscripts on $T(I,J)$ have been dropped to be consistent with what actually takes place in the computer program, namely, the immediate replacement of $\vec{T}_J^{(m-1)}$ by $\vec{T}_J^{(m)}$ once it is computed.

Of all the numbers a_i, b_i and c_i, only a_{NY} depends on the fact that computations are being carried out on the second vertical and at the mth iterate. Thus, if some other vertical, other than the last, were examined, the only changes that would occur in the coefficients in (B18) are as follows:

(1) a_{NY} is replaced by its correct value.

(2) $T_o + T(I,3)$ is replaced by $T(I,J - 1) + T(I,J + 1)$, $I = 1 \ldots NY$.

Therefore, if the previous system is solved by the elimination of unknowns, it is seen that as one proceeds from vertical to vertical and from iteration to iteration, the same arithmetic operations are performed on the same members with the same ratios (μ_i) appearing repeatedly (at least so far as the left-hand sides are concerned). Even for the right-hand sides the same operations are being performed with the same ratios (μ_i) as with the left-hand sides, but the operations are performed on numbers that depend on J and m. It is therefore advantageous to compute and store these μ_i ratios before any iterations are performed. It is this saving of the μ_i along with the modified a_i that has been referred to previously by "triangularizing of $\mathscr{B}_2$" (block 2 of fig. 10). Applying the previously mentioned operations and μ_i ratios to the iteration- and vertical-dependent right-hand sides (blocks 4 and 5 of fig. 10) leads to a reduced system of equations, the last of which involves only z_{NY} (block 6). This is then substituted into the preceding (modified) equation, which involves it with z_{NY-1} and the process continues backwards (in I) to z_1 (blocks 7 and 8). The values for the temperatures on this second vertical are then replaced by the new values (block 9):

$$T(I,2) + \omega[z_I - T(I,2)] \qquad I = 1 \ldots NY$$

Numerical experiments at Lewis indicate that there is an optimum value ω_b for ω, as in the case of equations that are all linear, where an a priori value can be given. For example, for a case where $NDYF = 4$, $NDYC = 2$, $NDX = 100$, $L = 0.1333$, $t_{cu} = t_{ss} = 0.0004167$, $k_{ss} = k_{cu} = 210$, $T_0 = 2337$, $\epsilon = 0.9$, and $\sigma = 0.1713 \times 10^{-8}$, it is found that ω_b near 1.96 gives a relative residual error

$$\frac{|\text{heat in} - \text{heat out}|}{\text{heat out}}$$

near 0.0001 in less than 300 iterations. This is a practicable convergence criterion for the problem at hand and is so used in the computer program (block 11 of fig. 10).

Here

$$\text{heat in} = -\int_{\substack{\text{Left} \\ \text{end}}} k \frac{\partial T}{\partial n} \, ds$$

$$\text{heat out} = -\int_{\substack{\text{Radiating} \\ \text{boundary}}} k \frac{\partial T}{\partial n} \, ds = \int \epsilon \sigma T_{ss}^4 \, ds$$

Trapezoidal integration is used to be consistent with the finite-difference equations. These experiments also indicate that for $\omega < \omega_b$ heat in increases monotonically to meet heat out, which is decreasing as m increases if $T^{(0)}(I,J)$ is chosen to be T_0 everywhere.

The program was converted to double precision after it was found that the large aspect ratio of the cells of the grid led to appreciable loss of significance. The program takes less than 1 minute to carry out 400 iterations for cases similar to those mentioned previously.

REFERENCES

1. Lieblein, Seymour: Special Requirements on Power Generation Systems for Electric Propulsion. Electric Propulsion for Spacecraft. NASA SP-22, 1962, pp. 5-14.

2. Denington, Robert J.; LeGray, William J.; and Shattuck, Russell D.: Electric Propulsion for Manned Missions. Proc. AIAA and NASA Conf. on Eng. Problems of Manned Interplanetary Exploration, Palo Alto (Calif.), Sept. 30-Oct. 1, 1963, pp. 145-159.

3. Diedrich, James H.; and Lieblein, Seymour: Materials Problems Associated with the Design of Radiators for Space Powerplants. Power Systems for Space Flight. Vol. 11 of Progress in Astronautics and Aeronautics, Academic Press, 1963, pp. 627-653.

4. Osmun, William G.: Space Nuclear Power: SNAP-50/SPUR. Space/Aeronautics, vol. 42, no. 7, Dec. 1964, pp. 38-45.

5. Parker, Kenneth O.; and Stone, Robert A.: Spur High-Temperature Space Radiator. Power Systems for Space Flight. Vol. 11 of Progress in Astronautics and Aeronautics, Academic Press, 1963, pp. 505-533.

6. Plamondon, J. A.: Thermal Efficiency of Coated Fins. TR 34-227, Jet Prop. Lab., C.I.T., 1961. (See also Paper No. 61-WA-168, ASME, 1961.)

7. Stockman, Norbert O.; and Kramer, John L.: Effect of Variable Thermal Properties on One-Dimensional Heat Transfer in Radiating Fins. NASA TN D-1878, 1963.

8. Lieblein, Seymour: Analysis of Temperature Distribution and Radiant Heat Transfer Along a Rectangular Fin of Constant Thickness. NASA TN D-196, 1959.

9. Bartas, J. G.; and Sellers, W. H.: Radiation Fin Effectiveness. Jour. Heat Transfer (Trans. ASME), ser. C, vol. 82, no. 1, Feb. 1960, pp. 73-75.

10. Roudebush, William H.: Analysis of Discretization Errors for Differential Equations with Discontinuous Coefficients. Ph.D. Thesis, Case Inst. Tech., 1963.

11. Engeli, M.; Ginsburg, T.; Rutishauser, H.; and Stiefel, E.: Refined Iterative Methods for Computation of the Solution and the Eigenvalues of Self-Adjoint Boundary Value Problems. Birkhäuser, Verlag (Basel) 1959, pp. 9-23.

12. Varga, R. S.: Matrix Iterative Analysis. Prentice-Hall, Inc., 1962.

13. Scarborough, J. B.: Numerical Mathematical Analysis. Johns Hopkins Press, 1955.